

A comparative study of photon beam percentage depth dose of a recently installed varian vitalbeam linear accelerator at TMSS cancer center, Bangladesh

Abstract

The commissioning procedure and maintenance of safety precautions before the beam is hit the affected cells are the key factors for the success of external beam radiotherapy. The percentage depth dose (PDD), which must be measured before a linear accelerator (LINAC) is used clinically, is one of the crucial factors during commissioning. Measurements for PDDs were carried out in this study at TMSS Cancer Center, Bogura, Bangladesh, using a linear accelerator (Varian VitalBeam SN: 5199, machine completely new in Bangladesh) with 6MV, 10MV and 15MV photon energies for a set of 10 field sizes keeping the same conditions such as pressure, temperature, incremental step, direction, geometry, chamber voltage and polarity. Two ionization chambers CC13 (SN:18616) and CC04 (SN:18635) were used to measure PDDs for the linear accelerator utilizing 3D water phantom (SMARTSCAN) and IBA myQA Accept software. Using a TPS beam analysis tool, PDDs were calculated (Eclipse, Version: 16.1, Algorithm: AAA and PO). The measured PDD curves for 6MV, 10MV and 15MV photon beams with above mentioned field sizes and at SSD 100 cm were compared with the PDD curves of the British Journal of Radiology-25. The maximum depth doses (d_{max}) for reference field size $10 \times 10 \text{ cm}^2$ are 15.0 mm, 24.0 mm and 29.0 mm and the PDDs at 10 cm depth (D_{10}) are 66.80%, 73.55% and 77.14% for 6 MV, 10 MV and 15 MV photon energies respectively. The results for the maximum depth doses (d_{max}) and the PDDs at 10 cm depth (D_{10}) are determined to be within the limit. The measured PDD curves and the PDD curves of BJR-25 exhibit good agreement.

Keywords: Percentage Depth Dose, PDD, LINAC, Commissioning, Beam Characteristics etc.

Volume 11 Issue 4 - 2024

Md. Riadul Islam Chowdhury,¹ Md. Fajle Rabby,² Rubel Ahmed,² Mahmuda Akter,² Md. Motiur Rahman²

¹Department of CSE, Pundra University of Science & Technology, Bangladesh

²Department of Radiation Oncology Physics, TMSS Cancer Center, Bangladesh

Correspondence: Md. Riadul Islam Chowdhury, Department of Computer Science and Engineering, Pundra University of Science & Technology, Bogura, Bangladesh, Tel +88 0152 1482725, Email riadul.mric@gmail.com

Received: July 15, 2024 | **Published:** August 01, 2024

Introduction

Radiation therapy advanced quickly after Roentgen's invention of X-rays in 1895. Since then, advancements in X-ray production technology have focused on computerized beam delivery with intensity modulation.¹ Radiation generation with sophisticated apparatus, such as the linear accelerator (LINAC), has emerged as a useful tool for therapeutic purposes. Compared to conventional X-ray machines, the radiation produced by LINAC offers several benefits. Modern radiotherapy primarily uses radiation from medical LINACs, which have been concurrently developed. High-energy X-rays are modified by a LINAC to conform to the shape of a tumor, effectively killing cancer cells while sparing surrounding healthy tissues. Additionally, for the generation of electrons at relativistic velocities, high-power LINACs are also being promoted.²

Beyond a successful scientific process known as commissioning, which is carried out by a medical physicist, LINAC can be utilized for therapy. Before LINACs are employed in clinical settings, thorough measurements of dosimetric parameters are made during the commissioning process in order to validate the treatment planning system, which is exercised to determine the most appropriate radiation technique and treatment approach for each patient.^{3,4} Consequently, it is essential to acquire a minimal data set that includes output characterization, profile, and percentage depth dose (PDD) for a variety of field sizes.

This work evaluated basic dosimetric characteristics, alike PDD, with different field diameters for 6 MV, 10 MV, and 15 MV

beam energies. These measurements were carried out using the Varian VitalBeam linear accelerator in a 3D computer-controlled water phantom (SMARTSCAN) at TMSS Cancer Center, Bogura, Bangladesh. Assuring that, the analytically determined parameters stay constant during regular LINAC operation. The data collected during the LINAC's first commissioning can serve as standard information for therapeutic purposes.

Machinery and procedure

Machinery

The Varian VitalBeam (SN:5199), a double energy configuration linear accelerator capable of producing both photon beams of 6 MV, 10 MV, 15 MV and 6 MV FFF energies and electron beams of 4 MeV, 9 MeV, 12 MeV, 15 MeV and 18 MeV energies, was employed in this study. PDDs for photon energies of 6 MV, 10 MV, and 15 MV were measured using a 3D water phantom, CC13 ionization chamber (SN:18616) as a field chamber, CC04 ionization chamber (SN:18635) as a reference chamber, and IBA myQA Accept software version 1.6. Utilizing the Eclipse (Version: 16.1), an external treatment planning system, the PDD calculations were carried out.

PDD measurement

The central axis PDD measurement is an essential part in the commissioning process. The central axis dose distribution can be described by normalizing the dosage at any depth in relation to the dose at specified depth. PDD is the absorbed dose ratio along the beam's center axis, expressed as a percentage of the absorbed dose

at any given depth Q divided by the absorbed dose at a designated specified depth P. (Figure 1)

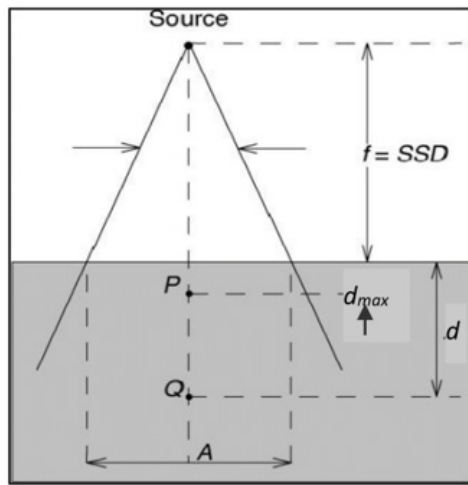


Figure 1 The setup for the measurement of PDD.

Thus, PDD is expressed as

$$PDD = \frac{D_Q}{D_P} \times 100\%$$

The absorbed dosage at any depth Q is denoted by D_Q , whereas the absorbed dose at a certain specified depth P is indicated by D_P .⁵

Experimental procedure

To measure PDD, phantom and a CC13 ionization chamber (SN:18616) must be placed at isocentric alignment with the LINAC system. The 3D water tank was matched with a spirit level, and the source to water surface distance was adjusted to 100 cm.

When the water surface was aligned with the chamber's effective point of measurement (EPOM), the ionization chamber in a PDD measurement was at zero depth. The IAEA dosimetry protocol states that a field chamber's EPOM is moved downstream by half of its inner radius (0.5r).⁶ This indicates that the chamber was moved downstream by the same amount and the zero was reset after the reference point was momentarily aligned with the water level. Just above the water's surface, in the measuring field's corner, a CC04 chamber was designated as the reference chamber. The PDD measurement phantom setup is depicted in Figure 2. In order to prevent water turbulence, PDD scanning was carried out continuously along the central axis of the phantom, starting at 310 mm depth and going all the way up to 0 mm depth. Beam scanning in 3D water phantom was controlled by IBA myQA Accept software.

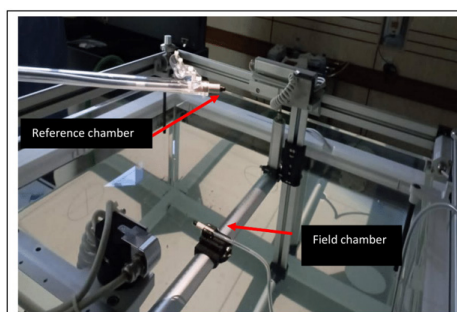


Figure 2 Phantom setup for PDDs measurements.

Ten square field sizes, namely 4 × 4, 6 × 6, 8 × 8, 10 × 10, 12 × 12, 15 × 15, 20 × 20, 30 × 30, 35 × 35, and 40 × 40 cm², were used to obtain the PDD curves. Because there is a dosimetric gap between multi-leaf collimators (MLCs), jaws were used to specify the field size rather than MLCs.⁷ The myQA Accept software was used to smooth out the curves. Finally, MS Excel software was used to calculate and plot the graph for this study.

Results and discussion

In this investigation, we explored the absorbed dosage as expressed by the percentage depth dose (PDD), which is dependent upon the following factors: depth (d), field size (A), and source to surface distance (SSD) (f). Plotting the observed PDD values for photon energies of 6 MV, 10 MV, and 15 MV across ten distinct field sizes we created PDD curves

Our research indicates that PDD increases as field size increases. This occurs because larger field sizes reduce photon scattering, leading to higher PDD for the same depth. An additional significant discovery is that the maximum depth dose (d_{max}) happens at particular depths below the surface. This is because, before depositing dose the secondary electrons must travel a distance. The PDD falls exponentially with depth after the maximum depth dose is reached. This is due to the complex interactions of photons with matter results a non-linear dose drop rates.

Additionally, our results show that as field size increases, the depth of maximum dose decreases. This happens because larger field sizes increase backscattering, which raises surface doses. For 6 MV, 10 MV, and 15 MV photon energies, we discovered that the maximal depth dosages are 15 mm, 24 mm, and 29 mm respectively. The average fall-off of dose (from D_{max} to D_{50}) per centimeter increases with smaller field sizes due to overlapping doses in these fields.

The surface dose (D_s), depth of 50% dosage (d_{50}), depth of maximum dose (d_{max}), and dose fall-off (D_{max} to D_{50}) per cent are displayed in Table 1. The PDD curves for different field sizes for beam energies of 6 MV, 10 MV and 15 MV are shown in Figures 3 to Figure 5, respectively.

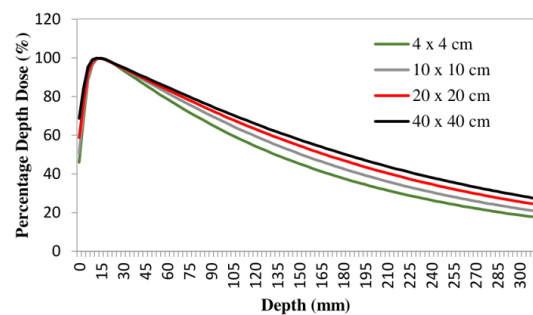


Figure 3 PDD curve for various FS with 6 MV photon beam.

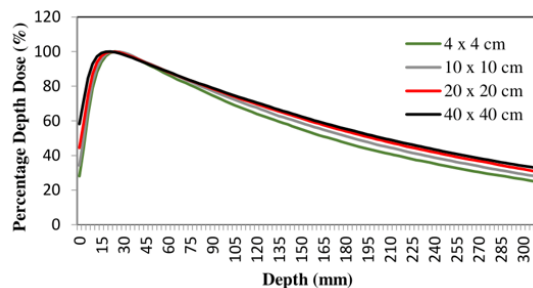


Figure 4 PDD curve for various FS with 10 MV photon beam.

Table 1 Surface dose (D_s), depth of maximum dose (d_{max}), depth of 50% dose (d_{50}) and decrease of dose (D_{max} to D_{50}) per cm for various FS of 6MV, 10 MV and 15 MV photon beams.

Field Size (cm ²)	Surface dose D_s (%)			Depth of max. dose d_{max} (cm)			Depth of 50% dose d_{50} (cm)			Fall of dose D_{max} to D_{50} (%cm ⁻¹)		
	6 MV	10 MV	15 MV	6 MV	10 MV	15 MV	6 MV	10 MV	15 MV	6 MV	10 MV	15 MV
4 × 4	45.9	27.9	24.3	1.60	2.50	2.95	13.45	16.90	18.65	4.22	3.47	3.18
6 × 6	47.7	29.8	26.6	1.55	2.50	2.90	14.15	17.80	18.95	3.97	3.27	3.12
8 × 8	49.2	31.9	28.9	1.55	2.45	2.90	14.75	18.15	19.60	3.79	3.18	2.99
10 × 10	50.7	34.1	32.8	1.50	2.40	2.90	15.20	18.45	20.05	3.67	3.11	2.91
12 × 12	51.7	36.1	34.3	1.50	2.40	2.70	15.50	18.85	20.20	3.55	3.04	2.86
15 × 15	55.4	39.3	36.8	1.50	2.35	2.60	16.05	19.15	20.55	3.43	2.98	2.79
20 × 20	58.7	44.3	44.1	1.50	2.30	2.50	16.80	19.80	20.95	3.27	2.86	2.71
30 × 30	65.1	55.7	55.2	1.45	2.20	2.15	17.75	20.45	21.20	3.07	2.74	2.62
35 × 35	67.5	58.0	56.9	1.45	1.85	2.05	18.05	20.75	21.45	3.01	2.65	2.58
40 × 40	68.7	58.1	58.6	1.45	1.80	1.95	19.25	21.05	21.65	2.81	2.60	2.54

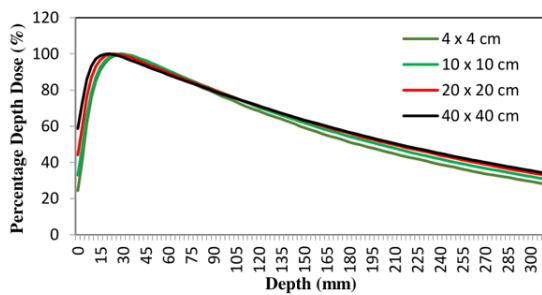


Figure 5 PDD curve for various FS with 15MV photon beam.

The surface doses for 6 MV, 10 MV, and 15 MV beam energies with a 10x10 cm² field size are 50.7%, 34.1%, and 32.8%, respectively, and the maximum dose is reached at depths of 1.5cm, 2.40cm, and 2.9 cm, respectively. This shows an average increase of doses of 31.7%, 27.5%, and 23.5% per cm until the maximum depth dose is reached. Figure 6 shows that the dosage increases quickly for all energies in the first few millimeters before progressively reaching its maximum value at the peak dose depth. It is evident that as photon energy increases, d_{max} rises and surface dose falls. Higher energy beams provide a larger dose at deeper depths and a lesser dose at the surface due to their increased penetrating capability.

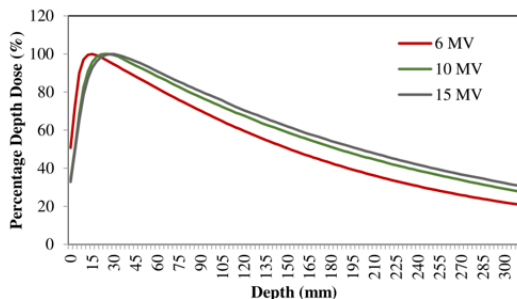


Figure 6 PDD curve with FS 10 × 10 cm² for various photon beams.

For various beam energies, a comparison was made between the depths of the maximum dose and depths of the 50% dose. Figure 7, which depicts the relative difference between d_{max} and d_{50} of photon

beams, illustrates how the disparity between these depths grows with increasing beam energy. The increased penetrating power of higher energy beams is indicated by the gap between the curves, which increases with photon energy. Therefore, when beam energy increases, the dosage fall per centimeter between these two depths (d_{max} to d_{50}) decreases. With a standard field size of 10×10 cm², the average dose reductions (D_{max} to D_{50}) per centimeter were determined 3.67%, 3.11%, and 2.91%, respectively. These values demonstrated a strong correlation with BJR-25. The mechanism of interaction between beams and matter causes the dosage drop rate following a nonlinear relationship. Because high-energy beams interact with matter differently than low-energy beams, their attenuation progression is significantly different.^{8,9,10}

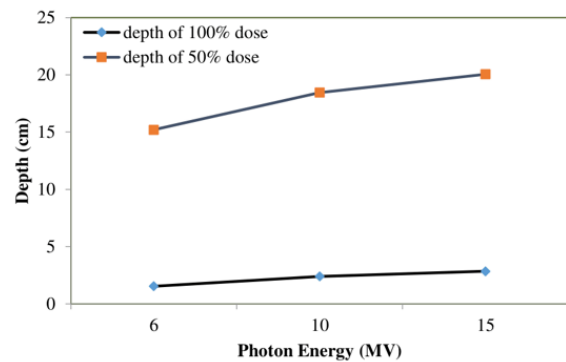


Figure 7 Depth of maximum dose and 50% dose with beam energy for FS 10 × 10 cm².

To validate the detected PDD, all PDDs obtained for 6MV, 10MV, and 15MV photon energies are compared to the standard PDD protocol, BJR-25. The comparison curves between the observed and BJR-25 PDD values for beam energies 6MV, 10MV, and 15 MV with the reference 10 × 10 cm² field size are displayed in Figures 8 to Figure 10, respectively. The comparison curves clearly show that the measured PDD and BJR-25 are match well.^{11,12} Table 2 displays the complete alignment of the measured values with BJR-25. Specifically, the dose at 10 cm depth (D_{10}), depth of 80% dosage (d_{80}), depth of maximum dose (d_{max}), and decline of dose (D_{max} to D_{50}) per centimeter are all in line with this standard protocol (BJR-25).

Table 2 Comparison between the measured data with the BJR 25 for 10 × 10cm² FS.

Energy	Observation	D ₁₀ (%)	d ₈₀ (cm)	d _{max} (cm)	Fall of dose D _{max} to D ₅₀ (%cm ⁻¹)
6MV	BJR 25	67.50	6.70	1.50	3.58
	Measured	66.80	6.60	1.50	3.67
10MV	BJR 25	73.00	8.00	2.30	3.18
	Measured	73.55	8.10	2.40	3.11
15MV	BJR 25	77.00	9.10	2.90	2.92
	Measured	77.14	9.10	2.90	2.91

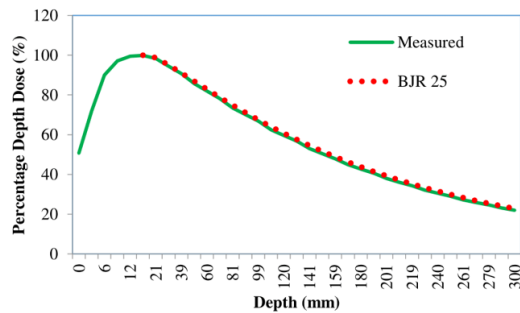


Figure 8 PDD curve with FS 10 × 10 cm² for 6MV photon beam.

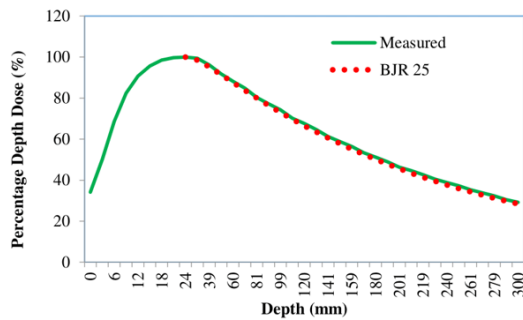


Figure 9 PDD curve with FS 10 × 10 cm² for 10MV photon beam.

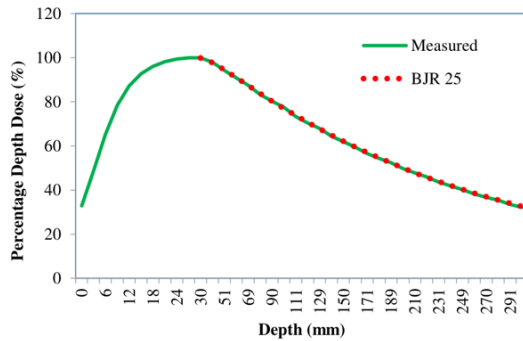


Figure 10 PDD curve with FS 10 × 10 cm² for 15MV photon beam.

For low energy (<10MV) photon beams the tolerance dose is up to 75% and for higher energy photon beams the tolerance dose is up to 89% at 10 cm depth as per AAPM TG-51.¹³⁻¹⁵ The PPD is obtained 66.80%, 73.55% and 77.14% for 6MV, 10MV and 15 MV photon energies respectively at 10 cm depth, which are within the limit mentioned in the AAPM TG-51 protocol.^{16,17}

Conclusion

This study highlights the significance of thorough dosimetric measurements in commissioning LINACs for clinical use. Accurate radiotherapy treatment planning relies heavily on understanding the PDD characteristics of medical LINACs, which are influenced by

factors such as depth, photon energy, field size, and SSD. The findings reveal that PDD increases with both photon energy and field size, while the maximum depth dose rises with beam energy but decreases with larger field sizes. The consistency of PDD data with established standards from BJR-25 and AAPM TG-51 for various photon beams underscores the reliability of these measurements. These insights are crucial for enhancing the precision and effectiveness of radiotherapy treatments, ultimately contributing to better patient outcomes.

Acknowledgments

The writers express their gratitude to the director of the TMSS Cancer Center in Bogura, Bangladesh, for providing them with the opportunity to work there. The authors also appreciate all of the Cancer Center's technical staff's cooperation during this procedure.

Conflicts of interests

All the authors declare there is no conflicts of interest.

References

- Podgorsak EB. Radiation oncology physics: a handbook for teachers and students. IAEA. 2005;103:370.
- Mittal VK, Verma RC, Gupta SC, *Introduction to nuclear and particle physics*. 2nd ed. 2011;247.
- Sahoo SK, Rath AK, Mukharjee RN, et al. Commissioning of a modern LINAC for clinical treatment and material research. *International Journal of Trends in Interdisciplinary Studies*. 2012;3:19.
- Uday MH, Khatun R, Rahman M, et al. Dosimetric verification of radiotherapy treatment planning system at TMSS Cancer Center, Bogura, Bangladesh. *World Journal of Advanced Engineering Technology and Sciences*. 2023;10(2):120–126.
- Khan FM, Gibbons JP, *The physics of radiation therapy*. 5th ed.
- IAEA International Atomic Energy Agency. Absorbed dose determination in external beam radiotherapy: an international code of practice for dosimetry based on standards of absorbed dose to water. Technical Report Series no. 398, IAEA, Vienna. 2000.
- Md Rahman M, Md Rabby F, Akter M, et al. MLC transmission and dosimetric leaf gap measurement using CU values from integrated images of varian vitalbeam. LINAC. 2023.
- Rahman M, Shamsuzzaman M, Sarker M, et al. Dosimetric characterization of medical linear accelerator Photon and Electron beams for the treatment accuracy of cancer patients. *World Journal of Advanced Engineering Technology and Sciences*. 2021;3(1):041–059.
- Varatharaj C, Shwetha B, Reddy RB, et al. Physical characteristics of photon and electron beams from a radiotherapy accelerator. *International Journal of Medical Research and Review*. 2016;4(7).
- Roy SK, Das PK, Khatun R, Md. et al. Dosimetric Characteristics of 6 MV Medical Linac at BAEC. *International Journal of Medical Physics, Clinical Engineering and Radiation Oncology*. 2021;10:38–46.

11. Central axis depth dose data for use in radiotherapy. *BJR*. 1996;25:90.
12. Li XJ, Ye YC, Zhang YS, et al. Empirical modeling of the percent depth dose for megavoltage photon beams. *PLoS One*. 2022;17(1):e0261042.
13. Almond PR, Nath R, Biggs PJ, et al. AAPM's TG-51 protocol for clinical reference dosimetry of high-energy photon and electron beams. *Med Phys*. 1999;26(9):1847–1870.
14. Md Rahman M, Md Rabby F, Ahmed R, et al. Radiotherapy bunker shielding calculations and recommendations for structural design for high energy photon facilities. *J Rad Nucl*. 2023;8(3):201–208.
15. Shimozato T, Aoyama Y, Matsunaga T, et al. Beam characterization of 10-MV photon beam from medical linear accelerator without flattening filter. *J Med Phys*. 2017;42(2):65–71.
16. Kragl G, Wetterstedt S, Knäusl B, et al. Dosimetric characteristics of 6 and 10 MV unflattened photon beams. *Radiother Oncol*. 2009;93(1):141–146.
17. Beyer GP. Commissioning measurements for photon beam data on three TrueBeam linear accelerators, and comparison with Trilogy and Clinac 2100 linear accelerators. *J Appl Clin Med Phys*. 2013;14(1):4077.